Flexible and high-throughput simultaneous profiling of gene expression and chromatin accessibility in single cells

Volker Soltys[1*], Moritz Peters[1], Dingwen Su[1], Marek Kučka[1,2,], Yingguang Frank Chan[1,3]

1 Friedrich Miescher Laboratory of the Max Planck Society, 72076 Tübingen, Germany
2 Department of Translational Genomics, University of Cologne, 50931 Cologne, Germany
3 University of Groningen, Groningen Institute of Evolutionary Life Sciences, 9747 AG Groningen, Netherlands

* Corresponding authors
volker.soltys@tue.mpg.de; frank.chan@rug.nl

Abstract

Gene expression and chromatin accessibility are highly interconnected processes. Disentangling one without the other provides an incomplete picture of gene regulation. However, simultaneous measurements of RNA and accessible chromatin are technically challenging, especially when studying complex organs with rare cell-types. Here, we present easySHARE-seq, an elaboration of SHARE-seq, providing simultaneous measurements of ATAC- and RNA-seq within single cells, enabling identification of cell-type specific *cis*-regulatory elements (CREs). easySHARE-seq retains high scalability, improves RNA-seq data quality while also allowing for flexible study design. Using 19,664 joint profiles from murine liver nuclei, we linked CREs to their target genes and uncovered complex regulation of key genes such as *Gata4*. We further identify *de-novo* genes and *cis*-regulatory elements displaying zonation in Liver sinusoidal epithelial cells (LSECs), a challenging cell type with low mRNA levels, demonstrating the power of multimodal measurements. EasySHARE-seq therefore provides a flexible platform for investigating gene regulation across cell types and scale.

Introduction

Gene expression and chromatin state combined influence fundamental processes such as gene regulation or cell fate decisions [1–3]. A better understanding of these mechanisms and their interactions will be a major step toward decoding developmental trajectories or reconstructing cellular taxonomies in both health and disease. However, to fully capture these complex relationships, multiple information layers need to be measured simultaneously. For example, prior studies have argued that chromatin state is often predictive of gene expression and can also prime cells toward certain lineage decisions or even induce tissue regeneration[4–6]. However, these studies depend on the computational integration of separately measured modalities. By assuming a shared biological state, this restricts the discovery of novel and potentially fine-scale differences and renders it challenging to identify the root cause of erroneous cell states[7].

The last decade has seen an explosive growth in single-cell methodologies, with new assays, increasing throughput and a suite of computational tools[8]. Most non-commercial high-throughput methodologies rely on combinatorial indexing for single-cell barcoding, where sequential rounds of barcodes combine to create unique cellular barcode combinations [9,10]. Compared to single-modality assays, multi-omic technologies, which capture two or more information layers, are relatively new. Therefore, they are still limited in sensitivity and throughput and commercial kits can be expensive such that multi-omic studies tend to have limited sample sizes [11,12].

To address these problems, we built upon a previously developed protocol called SHARE-seq[13] and developed easySHARE-seq, a protocol for simultaneously measuring gene expression and chromatin accessibility within single cells using combinatorial indexing. Major improvements include easySHARE-seq's barcoding framework, which allows for expanded and flexible study design, all while being compatible with standard Illumina sequencing, thereby removing economic hurdles. Importantly, easySHARE-seq retains the scalability and improves upon RNA-seq sensitivity of the original SHARE-seq protocol. Here, we used easySHARE-seq to profile 19,664 murine liver nuclei and show that we can recover high quality data in both RNA-seq and ATAC-seq channels, which are highly congruent and share equal power in classifying cell types. We then surveyed the *cis*-regulatory landscape of Liver Sinusoidal Endothelial Cells (LSECs), leveraging the simultaneous measurements of gene expression and chromatin accessibility and identified 40,957 links between expressed genes and nearby ATAC-seq peaks. Notably, genes with the highest number of links were enriched for transcription factors and regulators known to control important functions within LSECs. Lastly, we show that easySHARE-seq can be used to investigate micro-scale changes in accessibility and gene expression by identifying novel markers and open chromatin regions displaying zonation in LSECs. This technology improves our toolkit of multi-omic protocols needed for advancing our knowledge about gene regulation and cell fate decisions.

Results

easySHARE-seq reliably labels both transcriptome and accessible chromatin in individual cells

To develop a multi-omic single-cell (sc) RNA and scATAC-seq protocol that allows for flexible study design while being highly scalable, we built upon SHARE-seq[13] to create easySHARE-seq, which uses two rounds of ligation to simultaneously label cDNA and DNA fragments in the same cell (**Fig. 1A**). Due to a much more streamlined barcoding structure, easySHARE-seq allows 300bp sequencing of the insert. This longer read-length leads to a higher recovery of DNA variants, thus increasing the power to detect allele-specific signals or cell-specific variation, e.g., in hybrids or cancer cells[14].

To generate libraries, fixed and permeabilized cells or nuclei (we will use "cells" afterwards to refer to both) are transposed by Tn5 transposase carrying a custom adapter with a single-stranded overhang (**Fig. 1B**). Next, mRNA is reverse transcribed (RT) using a biotinylated poly(T) primer with an identical overhang. Subsequently, the cells are individually barcoded in two rounds of combinatorial indexing with 192 barcodes in each round, creating a total of 36,864 possible barcode combinations.The first barcode is ligated onto the already present overhang and itself contains a second single-stranded overhang, onto which the second barcode is ligated to. Importantly, in the easySHARE-seq design, we have kept the total length of the barcode within 17nt ("Index 1" read; **Fig. 1B, Suppl. Fig. 1A**), allowing for multiplexing of easySHARE-seq libraries with standard Illumina libraries. In contrast, in the original publication, SHARE-seq libraries required Index 1 lengths of 99nt, a highly custom configuration which would require a costly private sequencing run most of the time.

After barcoding, the cells are aliquoted into sub-libraries of approximately 3,500 cells each and reverse crosslinked. A streptavidin pull-down of the biotinylated RT-primer is performed to separate the cDNA molecules from the chromatin ("fragments"). Each sub-library is then prepared for sequencing and amplified using matched indexing primers to allow identification of paired cellular scRNA- and scATAC-seq profiles. By scaling up the numbers of sub-libraries, this barcoding strategy therefore allows for high-throughput experiments of hundreds of thousands of cells, only limited by the availability of indexing primers. For a detailed description of the flexibility of easySHARE-seq, instructions on how to modify and incorporate the framework into new designs as well as critical steps to assess when planning to use easySHARE-seq see Supplementary Notes.

To evaluate the accuracy and cell-specificity of the barcoding, we first performed easySHARE-seq on a mixed pool between human and murine cell lines (HEK and OP-9). This design allows us to identify two or more cells sharing the same barcode ('doublets'; **Fig. 1C**, left). After sequencing, we recovered a total of 3,808 cells. Both chromatin and transcriptome profiles separated well within each cell (**Fig. 1C**, middle), with cDNA showing a lower accuracy with increasing transcript counts, likely due to less precise read mapping. We identified a total of 124 doublets (**Fig, 1C**, right), which gives a final doublet rate of 6.34% factoring in the undetectable intra-species doublets. For comparison, a 10X Chromium Next GEM experiment with 10,000 cells has a doublet rate of ~7.9% (www.10xgenomics.com). Importantly, easySHARE-seq doublet rates can be lowered further by aliquoting fewer cells within each sub-library. To summarise, easySHARE-seq provides a high-throughput and flexibility framework for accurately measuring chromatin accessibility and gene expression in single cells.

Simultaneous scATAC-seq and scRNA-seq profiling in murine primary liver cells

To assess data quality and investigate the relationship between gene expression and chromatin accessibility, we focused on murine liver. The liver consists of a diverse set of defined primary cell types, ranging from large and potentially multinucleated hepatocytes to small non-parenchymal cell types such as Liver Sinusoidal Endothelial Cells[15] (LSECs).

We generated matched high-quality chromatin and gene expression profiles for 19,664 adult liver cells across four age-matched mice (2 male, 2 female), amounting to a recovery rate of 70.2% (28,000 input cells). Each nuclei had on average 3,629 UMIs and 2,213 fragments (74% of all RNA-seq reads were cDNA, 55.9% mean ATAC-seq fragments in peaks; **Suppl. Fig. 1B & D**). In terms of UMIs per cell, easySHARE-seq therefore out-performed other previously published multi-omic and representative single channel assays (**Fig. 2B**; see figure legend for tissue type and study). Consistent with nuclei as input material, the majority of cDNA molecules were intronic (69.6%, **Suppl. Fig. 1C & H**). Regarding DNA fragments per cell, easySHARE-seq performed similarly to other published multi-omic assays (**Fig. 2C**) and scATAC-seq libraries displayed the characteristic banding pattern with reads being highly enriched at transcription start sites (TSS; **Suppl. Fig. 1 E, F, H**).

To visualise and identify cell types, we first projected the ATAC- and RNA-seq modalities separately into 2D Space and then used Weighted Nearest Neighbor[16] (WNN) integration to combine both modalities into a single UMAP visualisation (**Fig. 2A)**. Importantly, the same cells independently clustered together in the scRNA- and scATAC-seq UMAPs, showcasing high congruence between the two modalities (**Suppl. Fig. 2A&B**). We then annotated previously published cell types based on gene expression of previously established marker genes [17,18]. Marker gene expression was highly specific to the clusters (**Fig. 2D, Suppl. Fig. 2F**) and we recovered all expected cell types (**Suppl. Fig.2C**). Importantly, the same cell types were identified using each modality independently, showcasing high congruence between the scATAC- and scRNA-seq modalities (**Fig. 2E**). Altogether, our results show that easySHARE-seq generates high quality joint cellular profiles of chromatin accessibility and gene expression within primary tissue, expanding our toolkit of multi-omic protocols.

Uncovering the cis-regulatory landscape of key regulators through peak-gene associations

As easySHARE-seq simultaneously measures chromatin accessibility and gene expression, it allows to directly investigate the relationship between them to potentially connect *cis*-regulatory elements (CREs) to their target genes. To do so, we adopted the analytical framework from Ma et al.[13], which queries if an increased expression within a cell is significantly correlated with chromatin accessibility at a peak while controlling for GC content and accessibility strength. Focusing on LSECs (1,501 cells), we calculated associations between putative CREs (pCREs, defined as peaks with a significant peak–gene association) and each expressed gene, considering all peaks within ± 500kb of the TSS. We identified 40,957 significant peak–gene associations (45% of total peaks, $P < 0.05$, FDR = 0.1) with 15,061 genes having at least one association (76.8% of all expressed genes, **Suppl. Fig. 3A,C**). In rare cases (2.9%), these pCREs were associated with five or more genes, which drop to 0.03% when considering only pCREs within ± 50 kb of a TSS (**Suppl. Fig. 3B,D**). These pCREs tended to cluster to regions of higher expressed gene density (2.15 mean expressed genes within 50kbp vs 0.93 for all global peaks) and their associated genes were enriched for biological processes such as mRNA processing, histone modifications and splicing (**Suppl. Fig. 3H**), possibly reflecting loci with increased regulatory activity.

We then ranked the genes based on their number of associated pCREs (**Fig. 2F**). Within the top 1% genes with the most pCRE associations were many key regulators and transcription factors. Examples include *Taf5,* which directly binds the TATA-box[19] and is required for initiation of transcription, or *Gata4,* which has been identified as the master regulator for LSEC specification during development as well as controlling regeneration and metabolic maturation of liver tissue in adult mice [20,21]. As such, it incorporates a variety of signals and its expression needs to be strictly regulated, which is reflected in its many pCREs associations (**Fig. 2H**). Similarly, *Igf1* also integrates signals from many different pCREs[22] (**Suppl. Fig. 3G**). Notably, pCRES are significantly enriched at transcription start sites (TSS), even relative to background enrichment (**Fig. 2G**).
To summarise, easySHARE-seq allows to directly investigate the relationship between chromatin accessibility and gene expression and identify putative *cis*-regulatory elements at genomic scale, even in small cell types with relatively low mRNA contents (**Suppl. Fig. 2D)**.

De Novo **identification of open chromatin regions and genes displaying zonation in LSECs**

We next investigated the process of zonation in LSECs. The liver consists of hexagonal units called lobules where blood flows from the portal vein and arteries toward a central vein [23,24] (**Fig. 3A)**. The central–portal (CP) axis is characterised by a morphogen gradient, e.g. from *Wnt2*, secreted by central vein LSECs, with the resulting micro-environment giving rise to spatial division of labour among hepatocytes [25–27]. Studying zonation in non-parenchymal cells such as LSECs is challenging as these are small cells with low mRNA content (**Suppl. Fig. 2D,E**), lying below the detection limit of current spatial transcriptomic techniques. As a result, only very few studies assess zonation in LSECs on a genomic level [28]. However, LSECs are critical to liver function as they line the artery walls, clear and process endotoxins, play a critical role in liver regeneration and secrete morphogens themselves to regulate hepatocyte gene expression [29–31], rendering their understanding a prerequisite for tackling many diseases.
We therefore asked if we can recover known zonation gradients and potentially identify novel marker genes and open chromatin regions displaying zonation. We noticed that LSECs clustered in a distinct linear pattern in our UMAP projection and therefore divided them into equal bins along UMAP2 coordinates (**Suppl. Fig. 4A**, number of cells per bin 80-260, median: 128). We then calculated mean normalised expression and mean normalised accessibility within each bin. This recovered gene expression and chromatin accessibility gradients for major known zonation marker genes[28] (**Fig. 3B,C**). For example, *Wnt2* expression decreased strongly along the CP axis as did chromatin accessibility of all three peaks at the *Wnt2* locus (**Fig. 3B**). We also recovered the zonation profiles for the majority of known pericentral (increasing along the CP-axis), periportal (decrease along the CP-axis) and non-monotonic markers (decrease toward both ends) as well as their associated chromatin regions (**Fig. 3C**). Gene expression zonation profiles can also be recovered by ordering LSECs along pseudotime (**Suppl. Fig. 4C,D**). In contrast, simply subclustering LSECs and comparing expression between these clusters was too broad for the assessment of zonation (**Suppl. Fig. 4A,B**).
Next, we sought to identify novel marker genes and open chromatin regions displaying zonation in LSECs based on the decrease or increase of mean expression or accessibility along the previously established bins. In total, we classified 153 genes and 381 open chromatin regions as pericentral and 209 genes and 465 open chromatin regions showed periportal zonation profiles (**Fig. 3D**). The list of markers contained many genes regulating epithelial growth and angiogenesis (e.g. *Efna1, Nrg2, Zfpm1, Zfpm2, Bmpr2*)[32–34], related to

regulating hepatocyte functions and communication (e.g. *Dll4, Foxo1, Sp1, Snx3*)[35–37] as well as immunological functions (e.g. *Sirt2, Cd59a)*[38,39]*,* suggesting that these processes show variation along the PC axis. As dysregulation of LSEC zonation is implicated in multiple illnesses such as liver cirrhosis or non-alcoholic fatty liver disease [40,41], these genes are potential new biomarkers for their identification and the open chromatin regions starting points for investigating the role of gene regulation in their emergence.

Discussion

Understanding complex processes such as gene regulation or disease states requires the integration of multiple layers of information. Here, we show that easySHARE-seq provides a high-quality, high-throughput and flexible platform for joint profiling of chromatin accessibility and gene expression within single cells. We show that both modalities are highly congruent with one another and we leverage their simultaneous measurements to identify peak–gene interactions and survey the *cis*-regulatory landscape of LSECs. We also show that easySHARE-seq can be used to assess micro-scale changes such as zonation in LSECs across both gene expression and chromatin accessibility. These cells have low mRNA content and we recovered zonation profiles of many transcription factors, which are often lowly expressed, further demonstrating the power of easySHARE-seq.

Besides improving upon RNA-seq data quality, we argue that easySHARE-seq has many advantages, especially in terms of the sequencing flexibility due to the barcode design, which can help remove hurdles for incorporating multi-omic single-cell assays into study designs. Combined with shorter experimental times (~12h total), easySHARE-seq might be particularly suited for studies where higher sample sizes are required or ones that rely on identification of genomic variants, e.g., in diverse, non-inbred individuals or in cancer. In terms of costs per cell, easySHARE-seq performs similarly to standard SHARE-seq with ~0.056 cents/cell, a fraction of the costs (<25%) of commercially available platforms, even before factoring in the specialized instrument costs. A comparison between technologies can be found in **Table 1**.

We envision easySHARE-seq as another technological step toward ultimately understanding gene regulation in health and disease, surveying *cis*-regulatory landscapes during differentiation and lineage commitment and determining genetic variants affecting those processes.

Figure 1

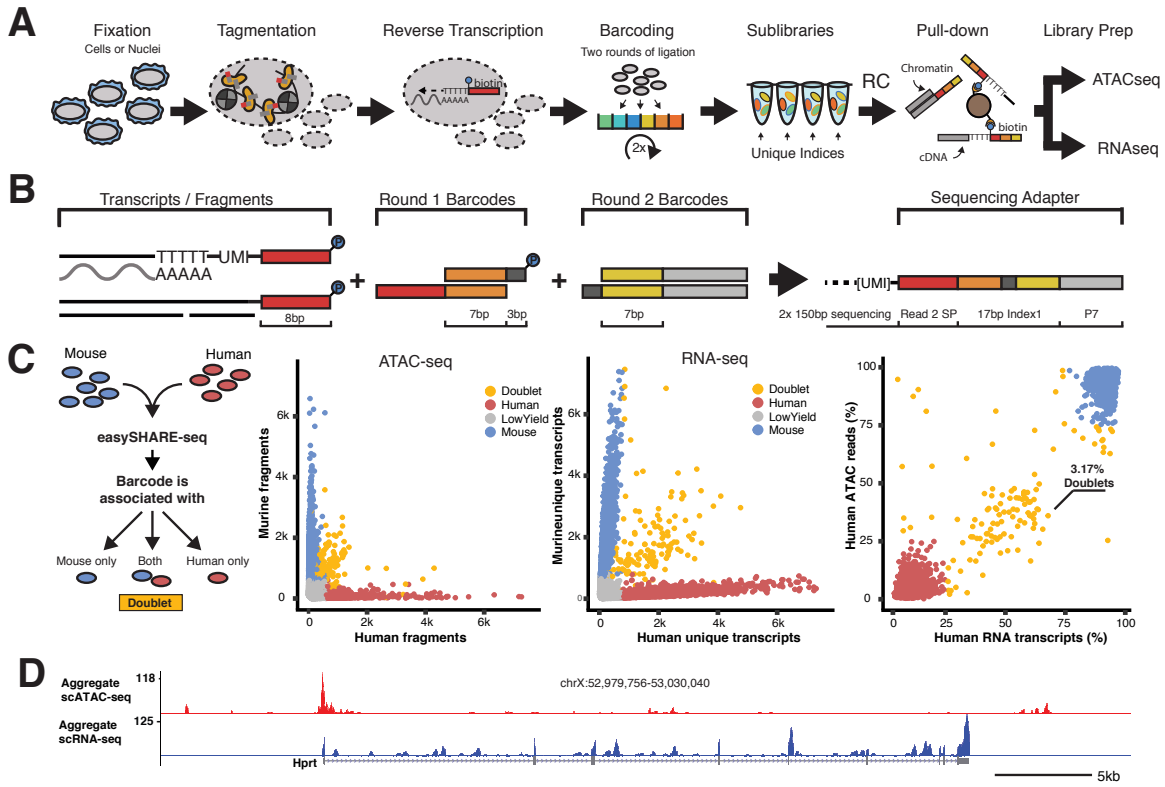

Figure 1: easySHARE-seq enables highly-accurate simultaneous scATAC-seq and scRNA-seq profiling

(A) Schematic workflow of easySHARE-seq.
(B) Generation and structure of the single-cell barcoding within Index 1.
(C) Principle of a species-mixing experiment. Cells are mixed prior to easySHARE-seq and sequences associated with each cell barcode are assessed for genome of origin (left panel). Unique ATAC fragments per cell aligning to the mouse or human genome (middle left). Cells are coloured according to their assigned origin (red: human; blue: mouse; orange: doublet). Middle right: Same plot but with RNA UMIs. Right: Percentage of ATAC fragments or RNA UMIs per cell relative to total sequencing reads mapping uniquely to the human genome. 3.17% of all observed cells classified as doublets. Accounting for same-species doublets, this results in a doublet rate of 6.34%.
(D) Aggregate chromatin accessibility (red) and expression-seq (blue) profile of OP-9 cells at the *Hprt* locus.

Figure 2

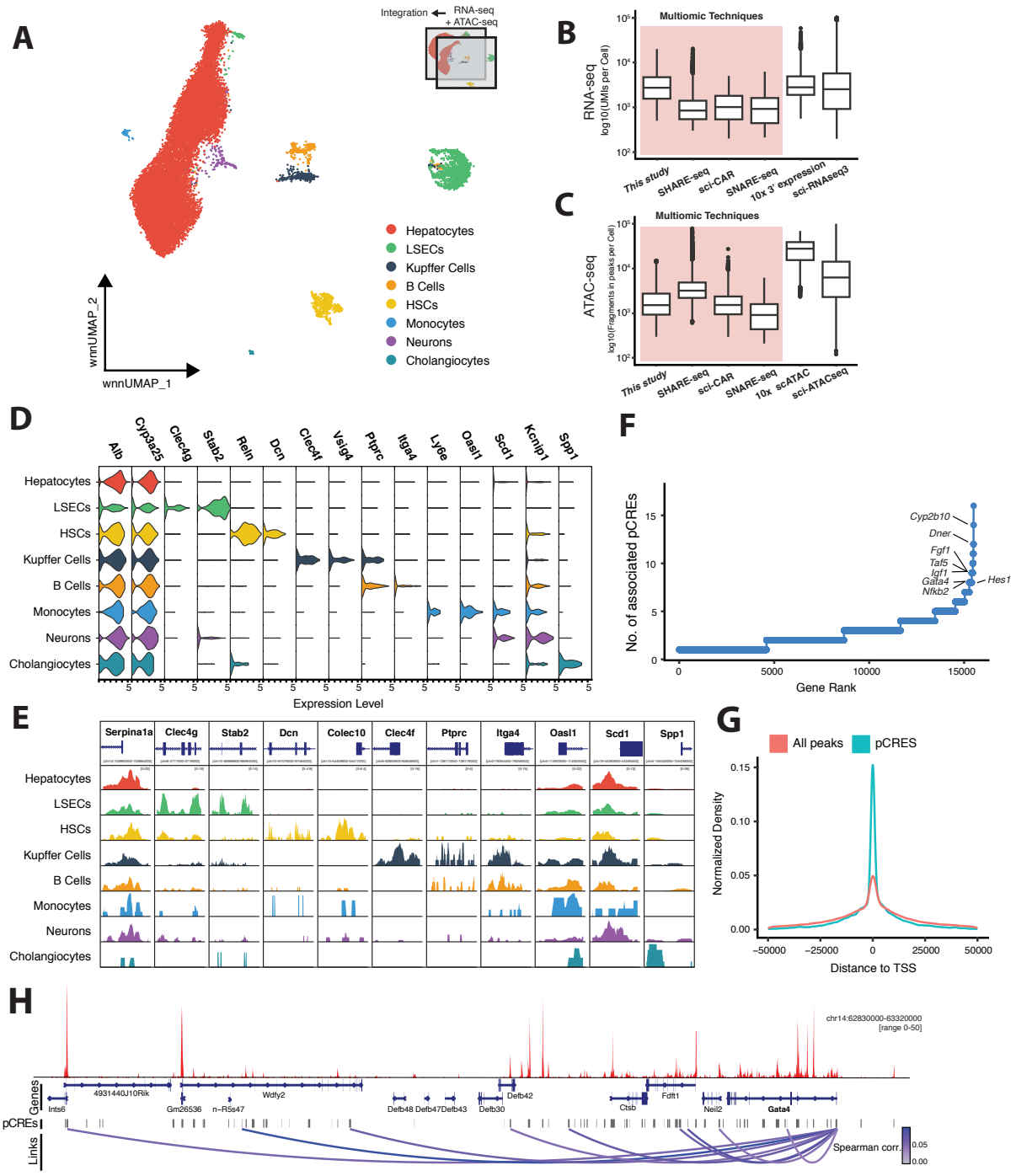
A
Integration
RNA-seq
+ ATAC-seq
Hepatocytes
LSECs
Kupffer Cells
B Cells
HSCs
Monocytes
Neurons
Cholangiocytes
wnnUMAP_2
wnnUMAP_1
B
Multiomic Techniques
RNA-seq
log10(UMIs per Cell)
This study
SHARE-seq
scl-CAR
SNARE-seq
10x 3' expression
scl-RNAseq3
C
Multiomic Techniques
ATAC-seq
log10(Fragments in peaks per Cell)
This study
SHARE-seq
scl-CAR
SNARE-seq
10x scATAC
scl-ATACseq
D
Alb
Cyp3a25
Clec4g
Stab2
Reln
Dcn
Clec4f
Vsig4
Ptprc
Itga4
Ly6e
Oasl1
Scd1
Kcnip1
Spp1
Hepatocytes
LSECs
HSCs
Kupffer Cells
B Cells
Monocytes
Neurons
Cholangiocytes
Expression Level
F
No. of associated pCREs
Gene Rank
Cyp2b10
Dner
Fgf1
Taf5
Igf1
Gata4
Nfkb2
Hes1
E
Serpina1a
Clec4g
Stab2
Dcn
Colec10
Clec4f
Ptprc
Itga4
Oasl1
Scd1
Spp1
Hepatocytes
LSECs
HSCs
Kupffer Cells
B Cells
Monocytes
Neurons
Cholangiocytes
G
All peaks
pCRES
Normalized Density
Distance to TSS
H
chr14:62830000-63320000
[range 0-50]
Genes
pCREs
Links
4931440J10Rik
Wdfy2
Gm26536
n-R5s47
Defb48
Defb47
Defb43
Defb30
Defb42
Ctsb
Fdft1
Neil2
Gata4
Spearman corr.

Figure 2: Joint expression and chromatin accessibility profiling in primary liver nuclei

(A) UMAP visualisation of WNN-integrated scRNAseq and scATACseq modalities of 19,664 liver nuclei. Nuclei are coloured by cell types.
(B) Comparison of UMIs/cell across different single-cell technologies. Red shading denotes all multi-omic technologies. Datasets are this study, SHARE-seq[13] (murine skin cells), sci-CAR[11] (murine kidney nuclei), SNARE-seq[12] (adult & neonatal mouse cerebral cortex nuclei), 10x 3' Expression[17] (murine liver nuclei) and sci-RNAseq3 [9](E16.5 mouse embryo nuclei).
(C) Comparison of unique fragments per cell across different single-cell technologies. Colouring as in (B). Datasets differing to (B) are 10x 3'scATAC[42] (murine liver nuclei) and sciATAC-seq[43] (murine liver nuclei).
(D) Normalised gene expression of representative marker genes per cell type.
(E) Aggregate ATAC-seq tracks at marker accessibility peaks per cell type.
(F) Genes ranked by number of significantly correlated pCREs ($P < 0.05$, FDR = 0.1) per gene (±500kbp from TSS) in LSECs. Marked are transcription factors & regulators within the top 1% of genes with a critical role in LSECs.
(G) Significantly correlated pCREs are enriched for TSS proximity. Normalised density of all peaks versus pCREs within ±50kbp of nearest TSS.
(H) Aggregate scATAC-seq track of LSECs at the *Gata4* locus and 500kbp upstream region. Loops denote pCREs significantly correlated with *Gata4* and are coloured by Spearman correlation of respective pCRE–*Gata4* comparison

Figure 3

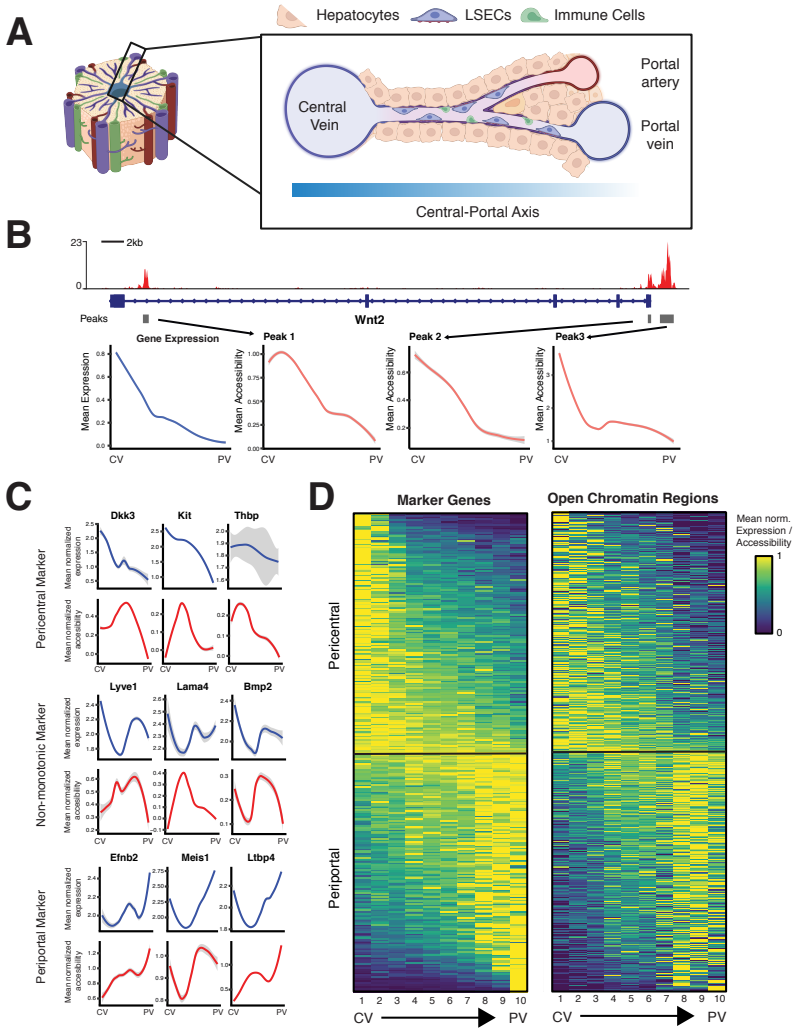

Figure 3: Zonation profiles in LSECs across gene expression and chromatin accessibility

(A) Schematic of a liver lobule. A liver lobule has a 'Central–Portal Axis' starting from the central vein to the portal vein and portal artery. The sinusoidal capillary channels are lined with LSECs.

(B) Changes along the Central–Portal Axis at the *Wnt2* locus. Top: Aggregate scATACseq profile (red) of LSECs at *Wnt2* locus. Grey bars denote identified peaks. Bottom: In blue, loess trend line of mean normalised *Wnt2* gene expression along the Central–Portal-Axis (central vein, CV; portal vein, PV; split into equal 10 bins). In red, loess trend line of mean normalised chromatin accessibility in peaks at the *Wnt2* locus along the CP-axis.

(C) Loess trend line of mean normalised expression (blue) and mean normalised accessibility along the Central–Portal axis for pericentral markers (top, increased toward the central vein, *Dkk3*, *Kit* and *Thbp*), non-monotonic markers (middle, increased between the veins, *Lyve1*, *Lama4* and *Bmp2*) and periportal markers (increased toward the portal vein, *Efnb2*, *Meis1* & *Ltbp4*)

(D) Left: Zonation profiles of 362 genes along the Central–Portal axis. Right: Zonation profiles of 846 open chromatin regions along the Central–Portal axis. All profiles are normalised by their maximum.

Table 1

Comparison of single-cell techniques

	Cost / Cell	Throughput	Multiomic?	Special equipment?	Std. sequencing?	Potential insert length?
This study	5.6 ct	> 200.000	Yes	No	Yes	> 200bp
SHARE-seq	4.33 ct	> 200.000	Yes	No	No	100bp
10x Multiome	25.8 ct	80.000	Yes	Yes	No	100bp
sci-RNA-seq3	1 ct	> 200.000	No	No	Yes	> 200bp

Table 1: Comparison between different single-cell technologies

Supplementary Figure 1

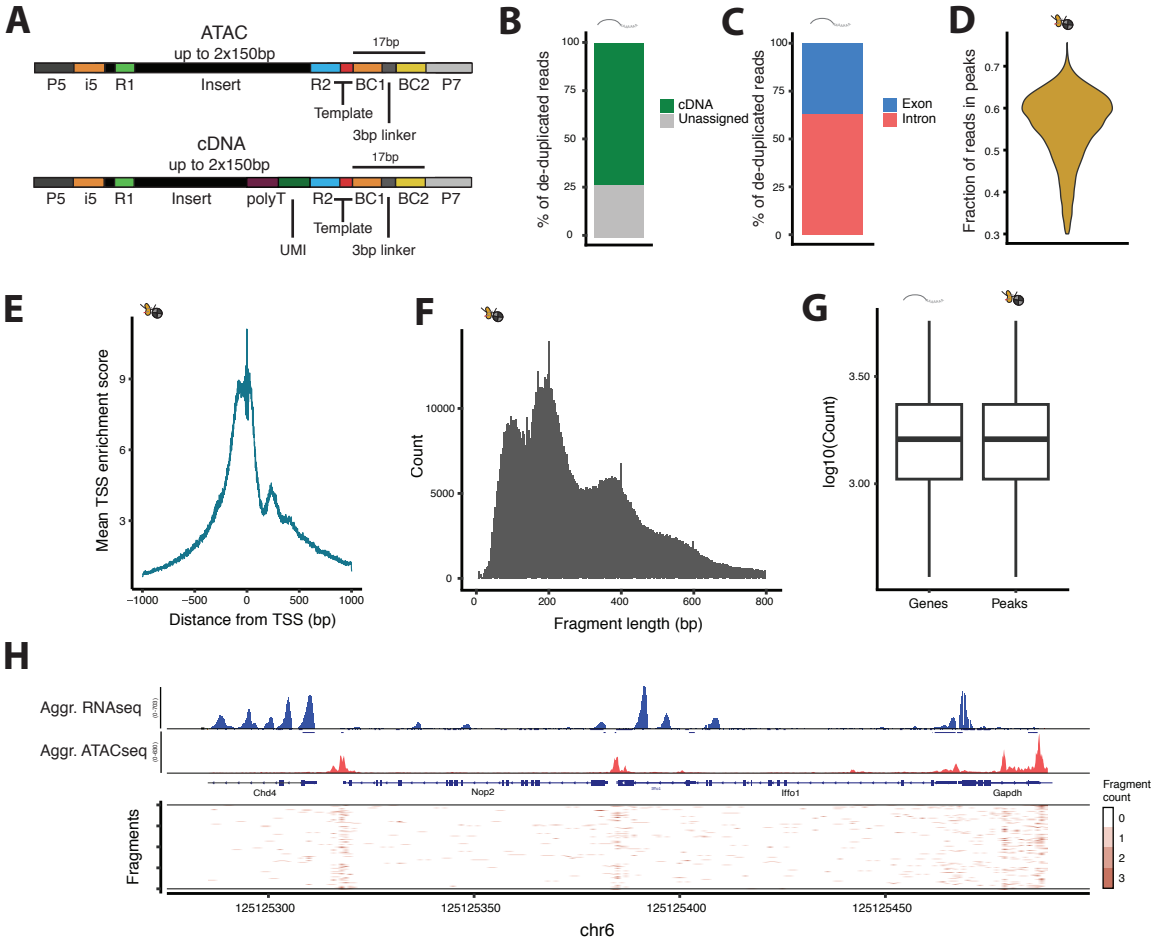

Supplementary Figure 1: Barcode structure and summary of quality control measures in liver nuclei

(A) Structure of a scATAC-seq and scRNA-seq sequencing read. Created with Biorender.com
(B) Percentage of total scRNAseq sequencing reads containing cDNA fragments.
(C) Percentage of de-duplicated scRNAseq sequencing reads overlapping an exon or intron.
(D) Distribution of fraction of reads in peaks (FRiP) per cell in the scATAC-seq data (mean: 0.55).
(E) Mean TSS enrichment score per cell in relation to distance from nearest TSS in the scATACseq data.
(F) Histogram of fragment length in scATAC sequencing reads
(G) Expressed genes and accessible peaks per cell (mean expressed genes: 1,798; mean accessible peaks: 1,983)
(H) Top: Aggregate scRNA-seq (blue) and scATAC-seq (red) of all liver nuclei at *Nop2/Iffo2/Gapdh* locus. Bottom: Chromatin accessibility profiles of 100 individual cells.

Supplementary Figure 2

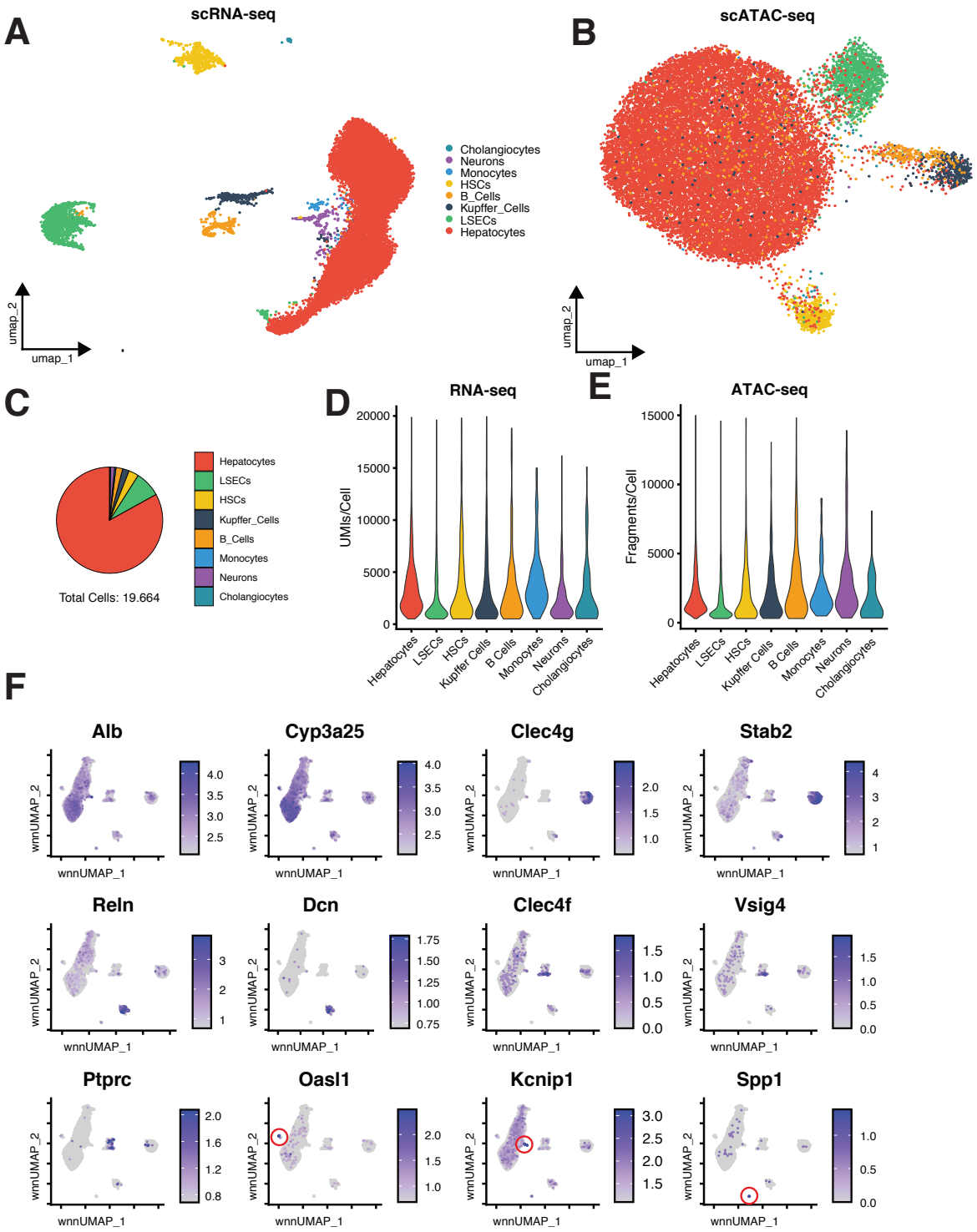

Supplementary Figure 2: easySHAREseq robustly separates cell types

(A) UMAP visualisation of merged and integrated scRNA-seq data. Nuclei are coloured according to their cell type.
(B) UMAP visualisation of merged and integrated scATAC-seq data. Nuclei are coloured according to their cell type.
(C) Fraction of cell types recovered relative to total cells
(D) Distribution of UMIs per cell split by cell type. Some cell types (e.g. LSECs) consistently yield less UMIs.
(E) Distribution of unique fragments per cell split by cell types. Some cell types (e.g. LSECs) consistently yield less fragments.
(F) WNN-UMAPs with cells coloured according to the mean expression strength of a given marker gene. Red circles indicate the position of the cell population showing elevated expression for this marker gene.

Supplementary Figure 3

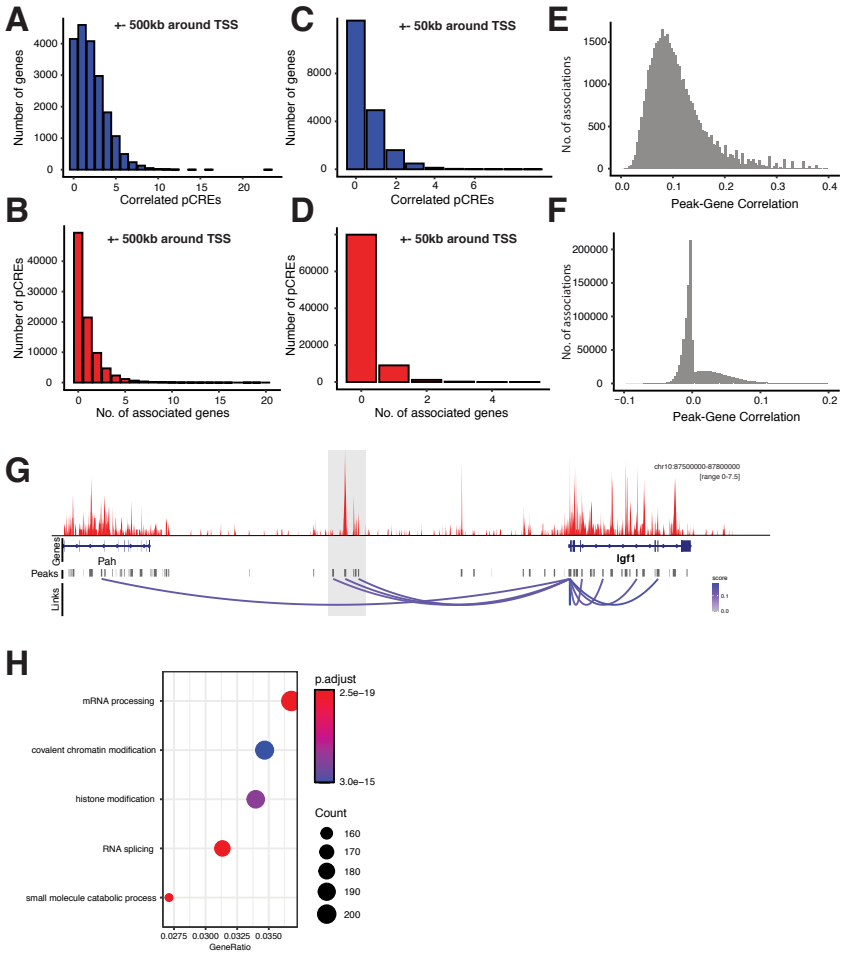

Supplementary Figure 3: Summary of peak–gene correlations

(A) Number of significantly correlated pCREs ($P < 0.05$, FDR = 0.1) per gene, considering all peaks ±500kbp of the TSS
(B) Number of genes a given pCREs is significantly correlated with ($P < 0.05$, FDR = 0.1), considering all peaks ±500kbp of the TSS
(C) Number of significantly correlated pCREs ($P < 0.05$, FDR = 0.1) per gene, considering all peaks ±50kbp of the TSS
(D) Number of genes a given pCREs is significantly correlated with ($P < 0.05$, FDR = 0.1), considering all peaks ±50kbp of the TSS
(E) Histogram of Spearman correlations of all significant peak–gene correlations ($P < 0.05$)
(F) Histogram of Spearman correlations of all non-significant peak–gene correlations ($P > 0.05$)
(G) Aggregate scATAC-seq track of LSECs at the *Igf1* locus and its upstream region. Loops denote significantly correlated pCREs with *Igf1* and are coloured by their respective Spearman correlation. Shaded grey area denotes potentially LSEC-specific *cis*-regulatory element regulating *Igf1* expression.
(H) Gene Ontology enrichment analysis of genes whose associated pCREs are associated with five or more genes.

Supplementary Figure 4

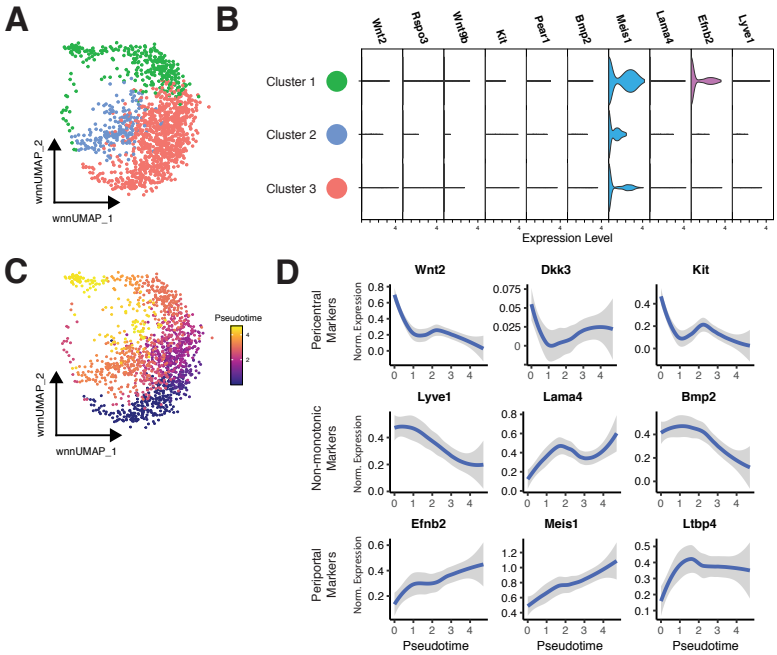

Supplementary Figure 4: Investigation of LSEC zonation

(A) Subclustering LSECs reveals three distinct clusters.
(B) Comparison of marker gene expression across the three identified LSEC subclusters does not allow for fine-scale cell-type assignments.
(C) Subclustered LSECs coloured by pseudotime.
(D) Loess-Curve of marker gene expression of pericentral, non-monotonic and periportal marker genes along pseudotime.

Methods

Animal Model & Tissue preparation

Mice

All animal experimental procedures were carried out under the licence number EB 01-21M at Friedrich Miescher Laboratory of the Max Planck Society in Tübingen, Germany. The procedures were reviewed and approved by the Regierungspräsidium Tübingen, Germany. Liver was collected from both male and female wild-type C57BL/6 and PWD/PhJ mice aged between 9 to 11 weeks.

Study design

From each strain, we generated easySHARE-seq libraries for one male and one female mice from each strain (four total). For each individual, we sequenced two sub-libraries, resulting in 8 easySHAREseq libraries.

Cell Culture

For the species-mixing experiment, HEK Cells were cultured in media containing DMEM/F-12 with GlutaMAX™ Supplement, 10% FBS and 1% Penicillin-Streptomycin (PenStrep) at 37°C and 5% CO_2. Cells were harvested on the day of the experiment by simply pipetting them off the plate and were then spun down for 5 min at 250G.
For the second cell line, murine OP9-DL4 cells were cultured in alpha-MEM medium containing 5% FBS and 1% PenStrep. On the day of the experiment, the cells were harvested by aspirating the media and adding 4 ml of Trypsin, followed by an incubation at 37°C for 5 min. Then, 5ml of media was added and cells were spun down for 5 min at 250G.
After counting both cell lines using TrypanBlue and the Evos Countess II, equal cell numbers were mixed.

Liver Nuclei

The liver was extracted, rinsed in HBSS, cut into small pieces, frozen in liquid nitrogen and stored in the freezer at -80 °C for a maximum of two weeks. On the day of the experiment, 1 ml of ice cold Lysis Solution (0.1% Triton-X 100, 1mM DTT, 10mMM Tris-HCl pH8, 0.1mM EDTA, 3mM $Mg(Ac)_2$, 3mM $CaCl_2$ and 0.32M sucrose) was added to the tube. The cell suspension was transferred to a pre-cooled Douncer and dounced 10x using Pestle A (loose) and 15x using Pestle B (tight). The solution was added to a thick wall ultracentrifuge tube on ice and topped up with 4ml ice cold Lysis Solution. Then 9 ml of Sucrose solution (10mM Tris-HCl pH8.0, 3mM $Mg(Ac)_2$, 3mM DTT, 1.8M sucrose) was carefully pipetted to the bottom of the tube to create a sucrose cushion. Samples were spun in a pre-cooled ultracentrifuge with a SW-28 rotor at 24,400rpm for 1.5 hours at 4 °C. Afterwards, all supernatant was carefully aspirated so as not to dislodge the pellet at the bottom and 1 ml ice cold DEPC-treated water supplemented with 10µl SUPERase & 15µl Recombinant RNase Inhibitor was added. Without resuspending, the tube was kept on ice for 20 min. The pellet was then resuspended by pipetting ~15 times slowly up and down followed by a 40 µm cell straining step. Counting of the nuclei using DAPI and the Evos Countess II was immediately followed up by fixation.

easySHARE-seq protocol

Preparing the barcoding oligonucleotides

There are two barcoding rounds in easySHARE-seq with 192 unique barcodes distributed across two 96-well plates in each round (see **Suppl. Table 1** for a full list of oligonucleotide sequences). Each barcode (BC) is pre-annealed as a DNA duplex for improved stability. The first round of barcodes contains two single-stranded linker sequences at its ends as well as a 5' phosphate group to ligate the different barcodes together. The first single-stranded overhang links the barcode to a complementary overhang at the 5' end of the cDNA molecule or transposed DNA molecule, which originates either from the RT primer or the Tn5 adapter. The second overhang (3bp) is used to ligate it to the second round of barcodes (**Fig.1B**). Each duplex needs to be annealed prior to cellular barcoding, preferably on the day of the experiment. No blocking oligos are needed.

The Round1 BC plates contain 10µl of 4µM duplexes in each well and Round2 BC plates contain 10µl of 6µM barcode duplexes in each well, all in Annealing Buffer (10mM Tris pH8.0, 1mM EDTA, 30mM KCl). Pre-aliquoted barcoding plates can be stored at -20 °C for at least three months. On the day of the experiment, the oligo plates were thawed and annealed by heating plates to 95 °C for 2 min, followed by cooling down the plates to 20 °C at a rate of -2 °C per minute. Finally, the plates were spun down. Until the annealed barcoding plates are needed, they should be kept on ice or in the fridge.

This barcoding scheme is very flexible and currently supports a throughput of ~350,000 cells (assuming 96 indexing primers) per experiment, limited only by sequencing cost and availability of indexing primer. The barcodes were designed to have at least a Hamming distance of 2. See Supplementary Notes for further details on the barcoding system and flexibility.

Tn5 *preparation*

Tn5 was expressed in-house as previously described [44]. Two differently loaded Tn5 are needed for easySHARE-seq, one for the tagmentation, loaded with an adapter for attaching the first barcodes (termed Tn5-B2S), and one for library preparation with a standard illumina sequencing adapter (termed Tn5-A-only). See Supplementary Table 1 for all sequences.

To assemble Tn5-B2S, two DNA duplexes were annealed: 20 µM Tn5-A oligo with 22 µM Tn5-reverse and 20 µM Tn5-B2S with 22 µM Tn5-reverse, all in 50 mM NaCl and 10mM Tris pH8.0. Oligos were annealed by heating the solution to 95 °C for 30 s and cooling it down to 20 °C at a rate of 2 °C/min. An equal volume of duplexes was pooled and then 200 µl of unassembled Tn5 was mixed with 16.5 µl of duplex mix. The Tn5 was then incubated at 37 °C for 1 hour, followed by 4 °C overnight. The Tn5 can then be stored at -20 °C. In our hands, Tn5 did not show a decrease in activity after 10 months of storage.

To assemble Tn5-A-only, 10 µM of Tn5-A and 10.5 µM Tn5-reverse was annealed using the same conditions as described above. Again, 200 µl of unassembled Tn5 was mixed with 16.5 µl of Tn5-A duplex and incubated at 37 °C for 1 hour, followed by 4 °C overnight. The Tn5 can then be stored for later and repeated use for more than 10 months at -20 °C.

We observed an increase in all Tn5 activity during the first months of storage, possibly due to continued transposome assembly in storage.

Fixation

One million liver nuclei ("cells" for short) were added to ice-cold PBS for 4 ml total. After mixing, 87 µl 16% formaldehyde solution (0.35%; for liver nuclei) or 25 µl 16% formaldehyde solution

(0.1%; for HEK and OP9 cells) was added and the suspension was mixed by pipetting up and down exactly 3 times with a P1000 pipette set to 700 µl. The suspension was incubated at room temperature for 10 min. Fixation was stopped by adding ice-cold Stop-Mix (224 µl 2.5M glycine, 200 µl 1M Tris-HCl pH8.0, 53 µl 7.5% BSA in PBS). The suspension was mixed exactly 3 times with a P1000 pipette set to 850 µl and incubated on ice for 3 min followed by a centrifugation at 500G for 5 min at 4°C. Supernatant was removed and the pellet was resuspended in 1 ml Nuclei Isolation Buffer (NIB; 10mM Tris pH8.0, 10mM NaCl, 2mM $MgCl_2$, 0.1% NP-40) and kept on ice for 3 min followed by straining the suspension with a 40 µm cell strainer. It was then spun down at 500G for 3 min at 4°C and re-suspended in ~100-200µl PBSi (1x PBS + 0.4 U/µl Recombinant RNaseInhibitor, 0.04% BSA, 0.2 U/µl SUPERase, freshly added), depending on the amount of input cells. Cells were then counted using DAPI and the Countess II and concentration was adjusted to 2M cells/ml using PBSi.

Tagmentation

In a typical easySHARE-seq experiment for this study, 8 tagmentation reactions with 10,000 cells each followed by 3 RT reactions were performed. This results in sequencing libraries for around 30,000 cells. To increase throughput, simply increase the amount of tagmentation and RT reactions accordingly. No adjustment is needed to the barcoding. Each tube and PCR strip until the step of Reverse Crosslinking was coated before use by rinsing it with PBS+0.5% BSA.

For each tagmentation reaction, 5 µl of 5X TAPS-Buffer, 0.25µl 10% Tween, 0.25µl 1% Digitonin, 3 µl PBS, 1 µl Recombinant RNaseInhibitor and 9µl of H2O was mixed. TAPS Buffer was made by first making a 1M TAPS stock solution in H_2O, followed by adjustment of the pH to 8.5 by titrating 10M NaOH. Then, 4.25ml H_2O, 500µl 1M TAPS pH8.5, 250µl 1M $MgCl_2$ and 5ml N-N-Di-Methyl-Formamide (DMF) was mixed on ice and in order. When adding DMF, the buffer heats up so it is important to be kept on ice. The resulting 5X TAPS-Buffer can then be stored at 4°C for short term use (1-2 months) or for long-term storage at -20°C (> 6 months).

Then, 5 µl of cell suspension at 2M cells/ml in PBSi was added to the tagmentation mix for each reaction, mixed thoroughly and finally 1.5µl of Tn5-B2S was added. The reaction was incubated on a shaker at 37°C for 30 min at 850 rpm. Afterwards, all reactions were pooled on ice into a pre-cooled 15ml tube. The reaction wells were washed with ~30 µl PBSi which was then added to the pooled suspension in order to maximize cell recovery. The suspension was then spun down at 500G for 3 min at 4°C. Supernatant was aspirated and the cells were washed with 200µl NIB followed by another centrifugation at 500G for 3 min at 4°C.

We only observed cell pellets when centrifuging after fixation and only when using cell lines as input material. Therefore, when aspirating supernatant at any step it is preferable to leave around 20-30µl liquid in the tube. Additionally, it is recommended to pipette gently at any step as to not damage and fracture the cells.

Reverse Transcription

As stated above, three tagmentation reactions were combined into one RT reaction. When increasing cells to more than 30,000 per RT reaction, we observed a steep drop in reaction efficiency.

The Master Mix for one RT reaction contained 3µl 100µM RT-primer, 2µl 10mM dNTPs, 6µl 5X MaximaH RT Buffer, 4.5µl 50% PEG6000, 1.5 µl H_2O, 1.5µl SUPERase and 1.66µl MaximaH RT. The RT primer contains a polyT tail, a 10bp UMI sequence, a biotin molecule and an adapter sequence used for ligating onto the first round of barcoding oligos.

The cell suspension was resuspended in 10µl NIB per RT reaction and added to the Master Mix for a total of 30µl. As PEG is present, it is necessary to pipette ~30 times up and down to ensure proper mixing. The RT reaction was performed in a PCR cycler with the following protocol: 52°C for 12 min; then 2 cycles of 8°C for 12s, 15°C for 45s, 20°C for 45s, 30°C for 30s, 42°C for 2min and 50°C for 3 min. Finally, the reaction was incubated at 52°C for 5 more minutes. All reactions were then pooled on ice into a pre-cooled and coated 15ml tube and the reaction wells were washed with ~40µl NIB, which was then added to the pooled cell suspension in order to maximise cell recovery. The suspension was then spun down at 500G for 3 min at 4°C. Supernatant was aspirated and the cells were washed in 150µl NIB and spun down again at 500G for 3min at 4°C. This washing step was repeated once more, followed by resuspension of the cells in 2ml Ligation Mix (400µl 10x T4-Buffer, 40µl 10% Tween-20, 1460µl Annealing Buffer and 100µl T4 DNA Ligase, added last).

Single-cell barcoding

Using a P20 pipette, 10µl of cell suspension in the ligation mix was added to each well of the two annealed Round1 BC plates, taking care as to not touch the liquid at the bottom of each well. The plates were then sealed, shaken gently by hand and quickly spun down (~ 8s) followed by an incubation on a shaker at 25°C for 30 min at 350 rpm. After 30 min, the cells from each well were pooled into a coated PCR strip using a P200 multichannel pipette set to 30µl. In order to pool, each row was pipetted up and down three times before adding the liquid to the PCR strip. After 8 columns were pooled into the strip, the suspension was transferred into a coated 5ml tube on ice. This process was repeated until both plates were pooled, taking care to aspirate most liquid from the plates. The cell suspension was then spun down for 3min at 500G at 4°C. Supernatant was aspirated and the cells were resuspended thoroughly in 2 ml new Ligation Mix. Now, 10µl of cell suspension was added into each well of the annealed Round2 barcoding plates using a P20 pipette, taking care as to not touch the liquid within each well. The plates were sealed, shaken gently by hand and spun down quickly followed by incubating them on a shaker at 25°C for 45 min at 350 rpm. The cells were then pooled again using the above described procedure into a new coated 15ml Tube. The cells were spun down at 500G for 3 min at 4°C. Supernatant was aspirated, the cells were washed with 150µl NIB and spun down again. Finally, the cells were resuspended in ~60µl NIB and counted. For counting, 5µl of cells were mixed with 5µl of NIB and 1x DAPI and counted on the Evos Countess II, taking the dilution into account. Sub-libraries of 3,500 cells were made and the volume was adjusted to 25µl by addition of NIB.

Using 3,500 cells results in a doublet rate of ~6.3%. The recovery rate of cells after sequencing depends on the input material (and QC thresholds), with cell lines recovering around 80% of input cells (~2,800-3,000 cells) and liver nuclei around 70% (~2,300-2,500 cells).

Reverse-Crosslinking

To each sub-library of 3,500 cells, 30µl 2x Reverse Crosslinking (RC) Buffer (0.4% SDS, 100mM NaCl, 100mM Tris pH8.0) as well as 5µl ProteinaseK was added. The sub-libraries were mixed and incubated on a shaker at 62°C for one hour at 800 rpm. Afterwards, they were transferred to a PCR cycler into a deep well module set to 62°C (lid to 80°C) for an additional hour. Afterwards, each sub-library was incubated at 80°C for 10 min and finally 5µl of 10% Tween-20 to quench the SDS and 35µl of NIB was added for a total volume of 100µl.

The lysates can be stored at this point at -20°C for at least two days, which greatly simplifies handling many sub-libraries at once. Longer storage has not been extensively tested.

Streptavidin Pull-Down

Each transcript contains a biotin molecule as the RT primers are biotinylated which is used to separate the scATAC-seq libraries from the scRNA-seq libraries. For each sublibrary, 50µl M280 Streptavidin beads were washed three times with 100µl B&W Buffer (5mM Tris pH8.0, 1M NaCl, 0.5mM EDTA) supplemented with 0.05% Tween-20, using a magnetic stand. Afterwards, the beads were resuspended in 100µl 2x B&W Buffer and added to the sublibrary, which were then shaken at 25°C for one hour at 900 rpm. Now all cDNA molecules are attached to the beads whereas transposed molecules are within the supernatant. The lysate was put on a magnetic stand to separate supernatant and beads.

It likely is possible to reduce the number of M280 beads in this step, significantly reducing overall costs. However, this has not been extensively tested.

scATAC-seq library preparation

The supernatant from each sub-library was cleaned up with a Qiagen MinElute Kit and eluted twice into 30µl 10mM Tris pH8.0 total. PCR Mix containing 10µl 5X Q5 Reaction Buffer, 1µl 10mM dNTPs, 2µl 10µM i7-TruSeq-long primer, 2µl 10µM Nextera N5XX Indexing primer, 4.5µl H2O and 0.5µl Q5 Polymerase was added (All Oligo sequences in **Suppl. Table 1**). Importantly, in order to distinguish the samples, each sub-library needs to be indexed with a different N5XX Indexing primer. The fragments were amplified with the following protocol: 72°C for 6 min, 98°C for 1 min, then cycles of 98°C for 10s, 66°C for 20s and 72°C for 45s followed by a final incubation at 72°C for 2 min. The number of PCR cycles strongly depends on input material (Liver: 17 PCR cycles, Cell Lines: 15 PCR cycles). The reactions were then cleaned up with custom size selection beads with 0.55X as upper cutoff and 1.4X as lower cutoff and eluted into 25µl 10mM Tris pH8.0. Libraries were quantified using the Qubit HS dsDNA Quantification Kit and run on the Agilent 2100 bioanalyzer with a High Sensitivity DNA Kit.

cDNA library preparation

The beads containing the cDNA molecules were washed three times with 200µl B&W Buffer supplemented with 0.05% Tween-20 before being resuspended in 100µl 10mM Tris ph8.0 and transferred into a new PCR strip. The strip was put on a magnet and the supernatant was aspirated. The beads were then resuspended in 50µl Template Switch Reaction Mix: 10µl 5X MaximaH RT Buffer, 2µl 100µM TS-oligo, 5µl 10mM dNTPs, 3µl Enzymatics RNaseIn, 15µl 50% PEG6000, 14µl H2O and 1.25µl MaximaH RT. The sample was mixed well and incubated at 25°C for 30 min followed by an incubation at 42°C for 90 min. The beads were then washed with 100µl 10mM Tris while the strip was on a magnet and resuspended in 60µl H_2O. To each well, 40µl PCR Mix was added containing 20µl 5X Q5 Reaction Buffer, 4µl 10µM i7-Tru-Seq-long primer, 4µl 10µM Nextera N5XX Indexing primer, 2µl 10mM dNTPs, 9µl H2O and 2µl Q5 Polymerase. The resulting mix can be split into two 50µl PCR reactions or run in one 100µl reaction. The PCR involved initial incubation at 98°C for 1 min followed by PCR cycles of 98°C for 10s, 66°C for 20s and 72°C for 3 min with a final incubation at 72°C for 5 min. Importantly, in order to distinguish the samples, each sub-library needs to be indexed with a different N5XX Indexing primer. The number of PCR cycles strongly depends on input material (Liver: 15 cycles, Cell lines: 13 cycles).

The PCR reactions were cleaned up with custom size selection beads using 0.7X as a lower cutoff (70µl) and eluted into 25µl 10mM Tris pH8.0. The cDNA libraries were quantified using the Qubit HS dsDNA Quantification Kit.

scRNA-seq library preparation

As the cDNA molecules are too long for sequencing (mean length > 700bp), they need to be shortened on one side. To achieve this, 25ng of each cDNA library was transferred to a new strip and volume was adjusted to 20µl using H_2O. Then 5µl 5X TAPS Buffer and 0.8µl Tn5-A-only was added and the sample was incubated at 55°C for 10 min. To stop the reaction, 25µl 1% SDS was added followed by another incubation at 55°C for 10 min. The sample was then cleaned up with custom size selection beads using a ratio of 1.3X and eluted into 30µl. Then 20µl PCR mix was added containing 10µl 5X Q5 reaction buffer, 1µl 10mM dNTPs, 2µl 10µM i7-Tru-Seq-long primer, 2µl 10µM Nextera N5XX Indexing primer (note: each sample needs to receive the **same** index primer as was used in the cDNA library preparation), 4.5µl H_2O and 0.5µl Q5 Polymerase. The PCR reaction was carried out with the following protocol: 72°C for 6 min, 98°C for 1 min, followed by 5 cycles of 98°C for 10s, 66°C for 20s and 72°C for 45s with a final incubation at 72°C for 2 min. Libraries were purified using custom size selection beads with a ratio of 0.5X as an upper cutoff and 0.8X as a lower cutoff. The final scRNA-seq libraries were quantified using the Qubit HS dsDNA Quantification Kit and run on the Agilent 2100 bioanalyzer with a High Sensitivity DNA Kit.

Sequencing

Both scATAC-seq and scRNA-seq libraries were sequenced simultaneously as they were indexed with different Index2 indices (N5XX). All libraries were sequenced on the Nova-seq 6000 platform (Illumina) using S4 2x150bp v1.5 kits (Read 1: 150 cycles, Index 1: 17 cycles, Index 2: 8 cycles, Read 2: 150 cycles). Libraries were partly multiplexed with standard Illumina sequencing libraries.

Custom Size selection beads

To make custom size selection beads, we washed 1ml of SpeedBeads on a magnetic stand in 1ml of 10mM Tris-HCl pH8.0 and re-suspended them in 50ml Bead Buffer (9g PEG8000, 7.3g NaCl, 500ul 1M Tris HCl pH8.0, 100ul 0.5M EDTA, add water to 50ml). The beads don't differ in their functionality from other commercially available ready-to-use size selection beads. They can be stored at 4°C for > 3 months.

Analysis

Gene annotations and Genomic variants

The reference genome and the Ensembl gene annotation of the C57BL/6J genome (mm10) were downloaded from Ensembl (Version GRCm38, release 102). Gene annotations for PWD/PhJ mice were downloaded from Ensembl. A consensus gene annotation set in mm10 coordinates was constructed by filtering for genes present in both gene annotations.

easySHARE-RNA-seq pre-processing

Fastq files were demultiplexed using a custom C-script, allowing one mismatch within each barcode segment. The reads were trimmed using cutadapt[48]. UMIs were then extracted from bases 1-10 in Read 2 using UMI-Tools[45] and added to the read name. Only reads with TTTTT at the bases 11-15 of Read 2 were kept (> 96%), allowing one mismatch. Lastly, the barcode was also moved to the read name.

Species-Mixing Experiments

RNA-seq reads were aligned to a composite hg38-mm10 genome using STAR[46]. The resulting bamfile was then filtered for uniquely mapping reads and reads mapping to chrM, chrY or unmapped scaffolds or containing unplaced barcodes were removed. Finally, the reads were deduplicated using UMItools[45]. ATAC-seq reads were also aligned to a composite genome using bwa[47]. Duplicates were removed with Picard tools and reads mapping to chrM, chrY or unmapped scaffolds were filtered out. Additionally, reads that were improperly paired or had an alignment quality < 30 were also removed.

The reads were then split depending on which genome they mapped to and reads per barcode were counted. Barcodes needed to be associated with at least 700 fragments and 500 UMIs in order to be considered a cell for the analysis. A barcode was considered a doublet when either the proportion of UMIs or fragments assigned to a species was less than 75%. This cutoff was chosen to mitigate possible mapping bias within the data.

easySHARE-RNA-seq processing and read alignment

We only used Read 1 for all our RNA-seq analyses as sequencing quality tends to drop after a polyT tail is sequenced in R2. Each sample was mapped to mm10 using the twopass mode in STAR[46] with the parameters --outFilterMultimapNmax 20 --outFilterMismatchNmax 15. We then processed the bamfiles further by moving the UMI and barcode from the read name to a bam flag, filtering out multimapping reads and reads without a definitive barcode. To determine if a read overlapped a transcript, we used featureCounts from the subread package[48]. UMI-Tools was used to collapse the UMIs of aligned reads, allowing for one mismatch and de-duplication of the reads. Finally, (single-cell) count matrices were created also using UMI-Tools.

easySHARE-ATAC-seq pre-processing and read alignment

Fastq files were demultiplexed using a custom C-script, allowing one mismatch within each barcode segment. The paired reads were trimmed using cutadapt[49] and the resulting reads were mapped to the mm10 genome using bwa mem[47]. Reads with alignment quality < Q30, unmapped, undetermined barcode, or mapped to mtDNA were discarded. Duplicates were removed using Picard tools. Open chromatin regions were called by subsampling the bamfiles from all samples to a common depth, merging them into a pooled bamfile and using the peak caller MACS2[50] with the parameters -nomodel -keep-dup -min-length 100. The count matrices as well as the FRiP score was generated using featureCounts from the Subread package[48] together with the tissue-specific peak set.

Filtering, Integration & Dimensional reduction of scRNAseq data

The count matrices were loaded into Seurat[51] and cells were then filtered for >200 detected genes, >500 UMIs and < 20.000 UMIs. The sub-libraries coming from the same experiment were then merged together and normalised. Merged experiments from the same species (one from male mouse, one from female mouse) were then integrated by first using SCTransform[52] to normalise the data, then finding common features between the two experiments using FindIntegrationAnchors() and finally integrated using IntegrateData(). Lastly, the integrated datasets from C57BL/6 and PWD/PhJ were again integrated using IntegrateData(). To visualise the data, we projected the cells into 2D space by UMAP using the first 30 principal components and identified clusters using FindClusters().

Filtering, Integration & Dimensional reduction of scATACseq data

Fragments per cell were counted using sinto and the resulting fragment file was loaded into Signac[53] alongside the count matrices and the peakset. We calculated basic QC statistics using base Signac and cells were then filtered for a FRiP score of at least 0.3, > 300 fragments, < 15.000 fragments, a TSS enrichment > 2 and a nucleosome signal < 4. Again, sublibraries coming from the same experiment were merged. We then integrated all four experiments (C57BL/6 & PWD/PhJ, one male & one female mouse each) by finding common features across datasets using FindIntegrationAnchors() using PCs 2:30 and then integrating the data using IntegrateEmbeddings(). To visualise the data, we projected the cells into 2D space by UMAP.

Weighted-Nearest-Neigbor (WNN) Analysis & Cell type identification

In order to use data from both modalities simultaneously, we created a multimodal Seurat object and used WNN[16] clustering to visualise and leverage both modalities for downstream analysis. Afterwards, we assigned cell cycle scores and excluded clusters consisting of nuclei solely in the G2M-phase (2 clusters, 121 nuclei total). Cell types were assigned via expression of previously known marker genes, which allows subsetting the data into cell types.

Calculating Peak–Gene Associations

Peak–gene associations were calculated following the framework described by Ma et al[13]. In short, Spearman correlation was calculated for every peak–gene pair within a +-500kb window around the TSS of the expressed gene. To obtain a background estimation, we used chromVAR[54] (*getBackgroundPeaks*()) to generate 100 background peaks matched in GC bias and chromatin accessibility but randomly distributed throughout the genome. We calculated the Spearman correlation between every background-gene comparison, resulting in a null distribution with known population mean and standard deviation. We then calculated the z-score for the peak–gene pair in question ((correlation - population mean)/ standard deviation) and used a one-sided z-test to determine the p-value. This functionality is also implemented in Signac under the function *LinkPeaks*(). Increasing the number of background peaks to 200, 350 or 500 for each peak–gene pair does not impact the results (*data not shown*).

Analysis of LSEC zonation markers

To analyse gene expression and chromatin accessibility along LSEC zonation, we subsetted our data for LSECs only, extracted expression values and wnnUMAP coordinates and binned the data along the wnnUMAP_2 axis into 10 equal sized bins. We then calculated the mean expression/accessibility for each gene/peak in each bin, excluding cells that contained a zero count. To identify novel marker genes, we excluded genes with low expression and calculated the moving average (for three bins) across the bins. We then required the moving average to continuously decrease (for pericentral marker genes) or increase (for periportal marker genes), allowing two exceptions. Lastly, we divided the means for each gene by their maximum to normalise the values. Identification of *cis*-regulatory elements displaying zonation effects had equal requirements.

Imputation of pseudotime was performed in Monocle3[55] with standard parameters. Gene expression was smoothed over both bins and pseudotime (separately) with local polynomial regression fitting (loess).

Gene Ontology Analysis

Gene Ontology Analysis was done using the R package clusterProfiler[56] with standard parameters.

Data Availability

All data can be accessed using the accession number GSE256434. All code used in data analysis is available at https://github.com/vosoltys/easySHARE_seq.git.

Acknowledgements

We thank members of the Chan and Jones lab for helpful discussions and critical reading of the manuscript. We are very grateful to Arnar Breevoort and Alex Pollen for sharing tissue preparation protocols and a very helpful research visit. We thank Sinja Mattes and all animal care takers at the Friedrich Miescher Laboratory for their work. We also thank the Genome Center in the Max Planck Institute for Biology for providing support.

Author Contributions

V.S. and M.P. developed the barcoding framework for easySHAREseq. V.S. developed the rest of the protocol and performed all experiments. V.S. did all computational analyses and wrote the manuscript. M.P., D.S., M.K. and Y.F.C. helped with experimental or computational support. All authors reviewed the manuscript.

Declaration of Interest

The authors declare no competing interests.

References

1. Anderson, E., Devenney, P. S., Hill, R. E. & Lettice, L. A. Mapping the Shh long-range regulatory domain. *Development* **141**, 3934–3943 (2014).
2. Nord, A. S. *et al.* Rapid and Pervasive Changes in Genome-wide Enhancer Usage during Mammalian Development. *Cell* **155**, 1521–1531 (2013).
3. Spitz, F. & Furlong, E. E. M. Transcription factors: from enhancer binding to developmental control. *Nat Rev Genet* **13**, 613–626 (2012).
4. Buenrostro, J. D. *et al.* Integrated Single-Cell Analysis Maps the Continuous Regulatory Landscape of Human Hematopoietic Differentiation. *Cell* **173**, 1535-1548.e16 (2018).
5. Zhang, C., Macchi, F., Magnani, E. & Sadler, K. C. Chromatin states shaped by an epigenetic code confer regenerative potential to the mouse liver. *Nat Commun* **12**, 4110 (2021).
6. Lara-Astiaso, D. *et al.* Chromatin state dynamics during blood formation. *Science* **345**, 943–949 (2014).
7. Stuart, T. *et al.* Comprehensive Integration of Single-Cell Data. *Cell* **177**, 1888-1902.e21 (2019).
8. Kashima, Y. *et al.* Single-cell sequencing techniques from individual to multiomics analyses. *Exp Mol Med* **52**, 1419–1427 (2020).
9. Martin, B. K. *et al.* Optimized single-nucleus transcriptional profiling by combinatorial indexing. *Nat Protoc* **18**, 188–207 (2023).
10. Rosenberg, A. B. *et al.* Single-cell profiling of the developing mouse brain and spinal cord with split-pool barcoding. *Science* **360**, 176–182 (2018).
11. Cao, J. *et al.* Joint profiling of chromatin accessibility and gene expression in thousands of single cells. *Science* **361**, 1380–1385 (2018).
12. Chen, S., Lake, B. B. & Zhang, K. High-throughput sequencing of the transcriptome and chromatin accessibility in the same cell. *Nat Biotechnol* **37**, 1452–1457 (2019).
13. Ma, S. *et al.* Chromatin Potential Identified by Shared Single-Cell Profiling of RNA and Chromatin. *Cell* **183**, 1103-1116.e20 (2020).
14. Lähnemann, D. *et al.* Eleven grand challenges in single-cell data science. *Genome Biology* **21**, 31 (2020).
15. Aizarani, N. *et al.* A Human Liver Cell Atlas reveals Heterogeneity and Epithelial Progenitors. *Nature* **572**, 199–204 (2019).
16. Hao, Y. *et al.* Integrated analysis of multimodal single-cell data. *Cell* **184**, 3573-3587.e29 (2021).
17. Su, Q. *et al.* Single-cell RNA transcriptome landscape of hepatocytes and non-parenchymal cells in healthy and NAFLD mouse liver. *iScience* **24**, 103233 (2021).
18. Han, X. *et al.* Mapping the Mouse Cell Atlas by Microwell-Seq. *Cell* **172**, 1091-1107.e17 (2018).
19. Chen, X. *et al.* Structural insights into preinitiation complex assembly on core promoters. *Science* **372**, eaba8490 (2021).
20. Winkler, M. *et al.* Endothelial GATA4 controls liver fibrosis and regeneration by preventing a pathogenic switch in angiocrine signaling. *J Hepatol* **74**, 380–393 (2021).
21. Géraud, C. *et al.* GATA4-dependent organ-specific endothelial differentiation controls liver development and embryonic hematopoiesis. *J Clin Invest* **127**, 1099–1114.
22. Lara-Diaz, V. *et al.* IGF-1 modulates gene expression of proteins involved in inflammation, cytoskeleton, and liver architecture. *J Physiol Biochem* **73**, 245–258 (2017).

23. Baratta, J. L. *et al.* Cellular Organization of Normal Mouse Liver: A Histological, Quantitative Immunocytochemical, and Fine Structural Analysis. *Histochem Cell Biol* **131**, 713–726 (2009).
24. Jungermann, K. & Kietzmann, T. Zonation of parenchymal and nonparenchymal metabolism in liver. *Annu Rev Nutr* **16**, 179–203 (1996).
25. Braeuning, A. *et al.* Differential gene expression in periportal and perivenous mouse hepatocytes. *The FEBS Journal* **273**, 5051–5061 (2006).
26. Planas-Paz, L. *et al.* The RSPO–LGR4/5–ZNRF3/RNF43 module controls liver zonation and size. *Nat Cell Biol* **18**, 467–479 (2016).
27. Wang, B., Zhao, L., Fish, M., Logan, C. Y. & Nusse, R. Self-renewing diploid Axin2+ cells fuel homeostatic renewal of the liver. *Nature* **524**, 180–185 (2015).
28. Halpern, K. B. *et al.* Paired-cell sequencing enables spatial gene expression mapping of liver endothelial cells. *Nat Biotechnol* **36**, 962–970 (2018).
29. Knolle, P. A. & Wohlleber, D. Immunological functions of liver sinusoidal endothelial cells. *Cell Mol Immunol* **13**, 347–353 (2016).
30. Smedsrød, B. Clearance function of scavenger endothelial cells. *Comparative Hepatology* **3**, S22 (2004).
31. Rafii, S., Butler, J. M. & Ding, B.-S. Angiocrine functions of organ-specific endothelial cells. *Nature* **529**, 316–325 (2016).
32. Theilmann, A. L. *et al.* Endothelial BMPR2 Loss Drives a Proliferative Response to BMP (Bone Morphogenetic Protein) 9 via Prolonged Canonical Signaling. *Arteriosclerosis, Thrombosis, and Vascular Biology* **40**, 2605–2618 (2020).
33. Russell, K. S., Stern, D. F., Polverini, P. J. & Bender, J. R. Neuregulin activation of ErbB receptors in vascular endothelium leads to angiogenesis. *American Journal of Physiology-Heart and Circulatory Physiology* **277**, H2205–H2211 (1999).
34. Vihanto, M. M. *et al.* Hypoxia up-regulates expression of Eph receptors and ephrins in mouse skin. *FASEB J* **19**, 1689–1691 (2005).
35. Shen, Z. *et al.* Delta-Like Ligand 4 Modulates Liver Damage by Down-Regulating Chemokine Expression. *Am J Pathol* **186**, 1874–1889 (2016).
36. Zellmer, S. *et al.* Transcription factors ETF, E2F, and SP-1 are involved in cytokine-independent proliferation of murine hepatocytes. *Hepatology* **52**, 2127–2136 (2010).
37. Dong, X. C. *et al.* Inactivation of Hepatic Foxo1 by Insulin Signaling Is Required for Adaptive Nutrient Homeostasis and Endocrine Growth Regulation. *Cell Metabolism* **8**, 65–76 (2008).
38. Wang, X., Yu, Y., Xie, H.-B., Shen, T. & Zhu, Q.-X. Complement regulatory protein CD59a plays a protective role in immune liver injury of trichloroethylene-sensitized BALB/c mice. *Ecotoxicology and Environmental Safety* **172**, 105–113 (2019).
39. Ren, H. *et al.* Sirtuin 2 Prevents Liver Steatosis and Metabolic Disorders by Deacetylation of Hepatocyte Nuclear Factor 4α. *Hepatology* **74**, 723 (2021).
40. Miyao, M. *et al.* Pivotal role of liver sinusoidal endothelial cells in NAFLD/NASH progression. *Laboratory Investigation* **95**, 1130–1144 (2015).
41. Su, T. *et al.* Single-Cell Transcriptomics Reveals Zone-Specific Alterations of Liver Sinusoidal Endothelial Cells in Cirrhosis. *Cellular and Molecular Gastroenterology and Hepatology* **11**, 1139–1161 (2021).
42. Nikopoulou, C. *et al.* Spatial and single-cell profiling of the metabolome, transcriptome and epigenome of the aging mouse liver. *Nat Aging* **3**, 1430–1445 (2023).
43. Cusanovich, D. A. *et al.* A Single-Cell Atlas of In Vivo Mammalian Chromatin Accessibility. *Cell* **174**, 1309-1324.e18 (2018).

44. Picelli, S. *et al.* Tn5 transposase and tagmentation procedures for massively scaled sequencing projects. *Genome Res.* **24**, 2033–2040 (2014).
45. Smith, T., Heger, A. & Sudbery, I. UMI-tools: modeling sequencing errors in Unique Molecular Identifiers to improve quantification accuracy. *Genome Res* **27**, 491–499 (2017).
46. Dobin, A. *et al.* STAR: ultrafast universal RNA-seq aligner. *Bioinformatics* **29**, 15–21 (2013).
47. Li, H. & Durbin, R. Fast and accurate short read alignment with Burrows–Wheeler transform. *Bioinformatics* **25**, 1754–1760 (2009).
48. Liao, Y., Smyth, G. K. & Shi, W. featureCounts: an efficient general purpose program for assigning sequence reads to genomic features. *Bioinformatics* **30**, 923–930 (2014).
49. Martin, M. Cutadapt removes adapter sequences from high-throughput sequencing reads. *EMBnet.journal* **17**, 10–12 (2011).
50. Zhang, Y. *et al.* Model-based Analysis of ChIP-Seq (MACS). *Genome Biology* **9**, R137 (2008).
51. Butler, A., Hoffman, P., Smibert, P., Papalexi, E. & Satija, R. Integrating single-cell transcriptomic data across different conditions, technologies, and species. *Nat Biotechnol* **36**, 411–420 (2018).
52. Hafemeister, C. & Satija, R. Normalization and variance stabilization of single-cell RNA-seq data using regularized negative binomial regression. *Genome Biology* **20**, 296 (2019).
53. Stuart, T., Srivastava, A., Madad, S., Lareau, C. A. & Satija, R. Single-cell chromatin state analysis with Signac. *Nat Methods* **18**, 1333–1341 (2021).
54. Schep, A. N., Wu, B., Buenrostro, J. D. & Greenleaf, W. J. chromVAR: inferring transcription-factor-associated accessibility from single-cell epigenomic data. *Nat Methods* **14**, 975–978 (2017).
55. Trapnell, C. *et al.* The dynamics and regulators of cell fate decisions are revealed by pseudotemporal ordering of single cells. *Nat Biotechnol* **32**, 381–386 (2014).
56. Yu, G., Wang, L.-G., Han, Y. & He, Q.-Y. clusterProfiler: an R Package for Comparing Biological Themes Among Gene Clusters. *OMICS: A Journal of Integrative Biology* **16**, 284–287 (2012).